

Numerical investigation of the dynamics of an axisymmetric rotor-stator flow

Artur Gesla

Devant le jury composé de :

Marc Avila

Full professor, Universität Bremen

Rapporteur

Denis Sipp

Directeur de recherche, Office National d'Études et de Recherches Aérospatiales

Rapporteur

Ivan Delbende

Maître de conférences HDR, Institut Jean le Rond d'Alembert, Sorbonne Université

Examinateur

Laurette Tuckerman

Directrice de recherche émérite, PMMH-CNRS, Sorbonne Université

Examinaterice

Laurent Martin Witkowski

Professeur des universités, Université Claude Bernard Lyon 1

Directeur de thèse

Yohann Duguet

Chargé de recherche HDR, LISN-CNRS, Université Paris-Saclay

Co-Directeur de thèse

Patrick Le Quéré

Directeur de recherche émérite, LISN-CNRS, Université Paris-Saclay

Co-Encadrant de thèse

Presentation plan

1 Introduction

- Motivation
- Flow configuration

2 Self-sustained regime

- Linear stability and Hopf branch
- Large amplitude chaotic branch and edge state

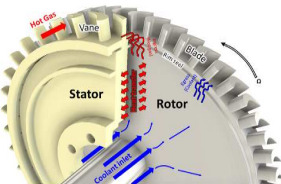
3 Noise-sustained regime

- Optimal forcing through resolvent analysis
- Noise response and comparison with experiments

4 Summary and outlooks

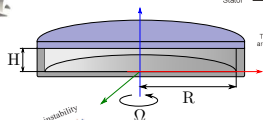
Introduction

Motivation

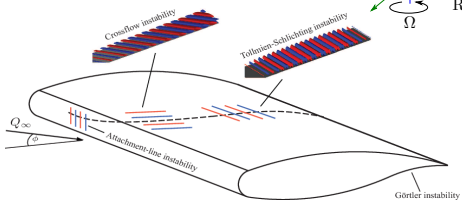


1.4 Rotor-stator spinning disc reactor

(Choi et al., Energy 2024)



(M. Meeuwse, PhD 2011)

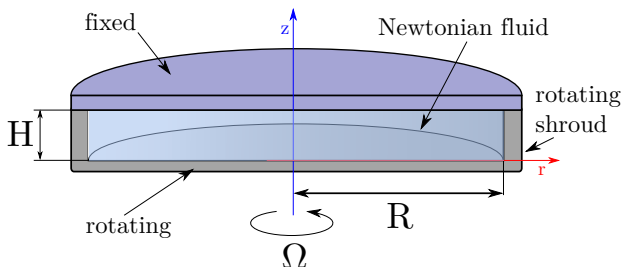


(D. Tempelmann, PhD 2011)

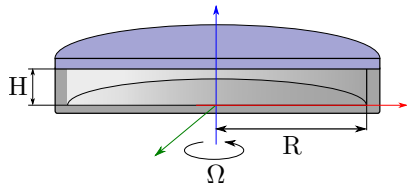


(J. Serpieri, PhD 2014)

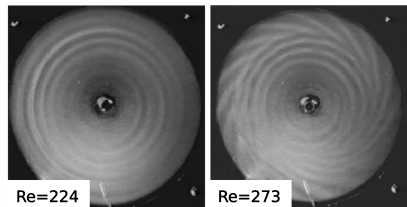
Flow set-up



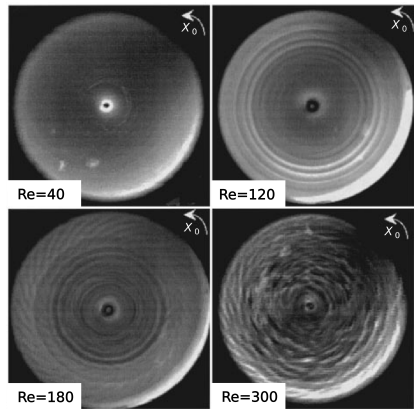
- flow of an incompressible fluid of viscosity ν
- characterised by:
 - Reynolds number: $Re = \Omega H^2 / \nu$ ($Re_R = \Omega R^2 / \nu$)
 - Aspect ratio $\Gamma = R/H$



$$Re = \Omega H^2 / \nu, \text{ aspect ratio } \Gamma = R/H$$



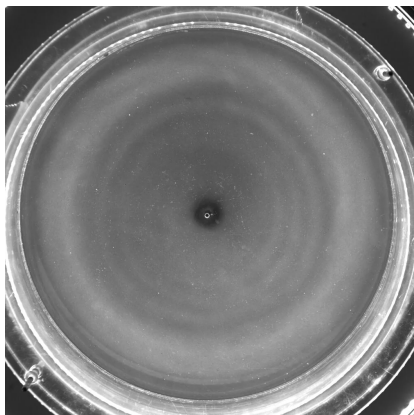
Circular and spiral rolls,
 $R/H = 8.75$,
 Schouveiler *et al.*, JFM 2001
 IRPHE, Marseille



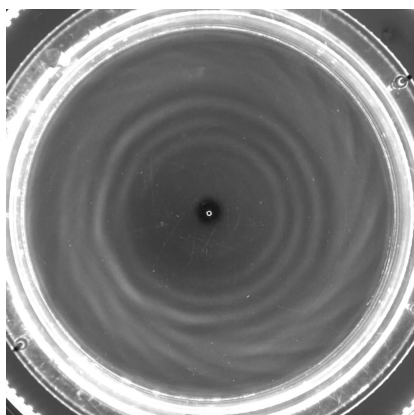
Circular and spiral rolls,
 $R/H = 20.9$,
 Gauthier *et al.*, JFM 1999,
 FAST, Orsay

Focus of this study: $R/H = 10$

Circular rolls $Re=205$:

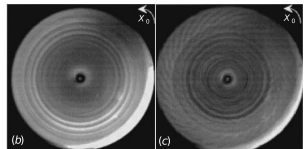
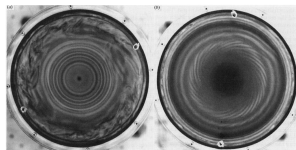


Circular and spiral rolls $Re=225$:



Videos: Kalliroscope visualisations prepared in the scope of an internship of Florence Brunox (2024, LMFA, INSA Lyon), Valery Botton and Simon Dagois-Bohy and Laurent Martin Witkowski (LMFA, Lyon, set-up FAST)

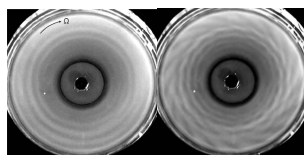
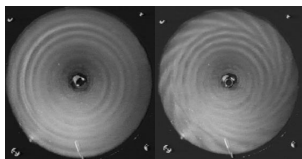
History (experiments)



(Savas, Pof 1983)

(Savas, JFM 1987)

(Gauthier et al., JFM 1999)

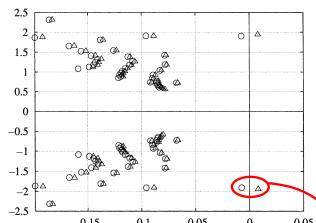


(Schouweiler et al., JFM 2001)

(Poncet et al., Pof 2009)

Experiments: circular rolls followed by spirals at higher Re

History (2D numerics) - axisymmetric study of Daube & Le Quéré (2001)



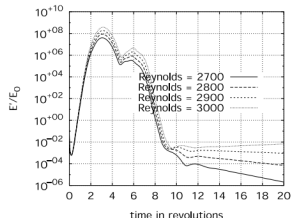
Linear instability $Re=3000$



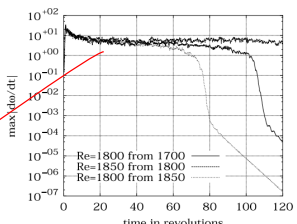
Most unstable eigenmode



Chaotic regime



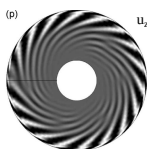
Large non-normal growth



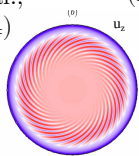
Subcritical regime $Re=1800$

History (3D numerics)

Direct numerical simulations

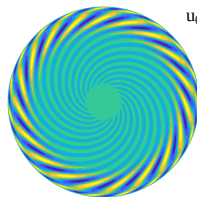


(Serre et al.,
Pof 2004)



(Lopez et al., Pof 2009)

Linear stability analysis

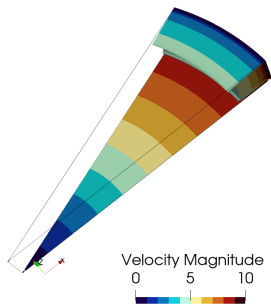


(Gelfgat., Fluid Dyn. Res. 201

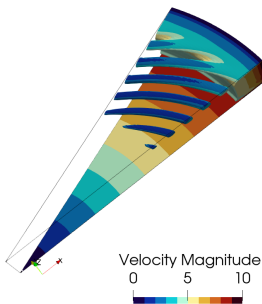
Numerics: Spirals result from a supercritical Hopf bifurcation,
but no sign of circular rolls.

DNS runs ($L_r = 10$, $L_\theta = 2\pi/16$, $L_z = 1$)

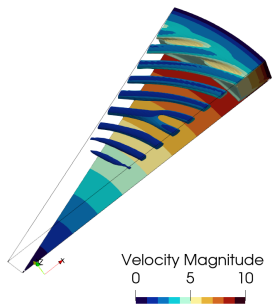
Re<Re_c, Time: 197.51



Re~Re_c, Time: 197.51

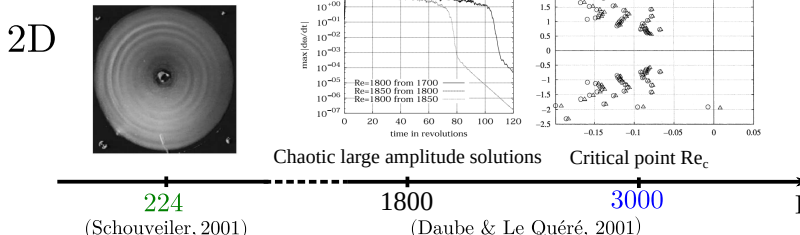
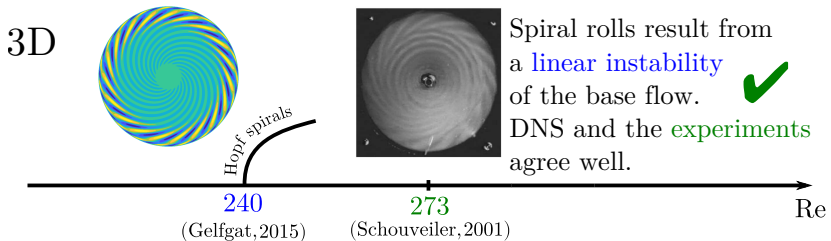


Re>Re_c, Time: 197.51

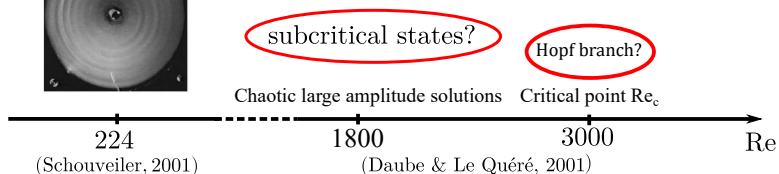
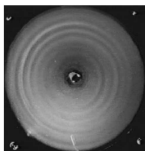


Isosurface of const. Q-criterion colored by the velocity magnitude
(Sunfluidh code, Y. Fraigneau, LISN; mesh: $N_r = 128$, $N_\theta = 32$,
 $N_z = 64$).

Possible scenarios for the axisymmetric rolls



2D



Hunt for the circular rolls:

- are they a subcritical self-sustained state?
- are they connected to the critical point of Daube & Le Quéré?

Objective:

- complete the bifurcation diagram of self-sustained states

Self-sustained regime

1 Introduction

- Motivation
- Flow configuration

2 Self-sustained regime

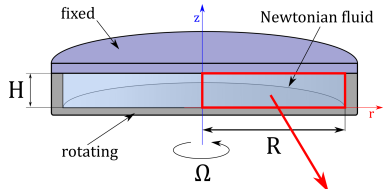
- Linear stability and Hopf branch
- Large amplitude chaotic branch and edge state

3 Noise-sustained regime

- Optimal forcing through resolvent analysis
- Noise response and comparison with experiments

4 Summary and outlooks

2D Base flow

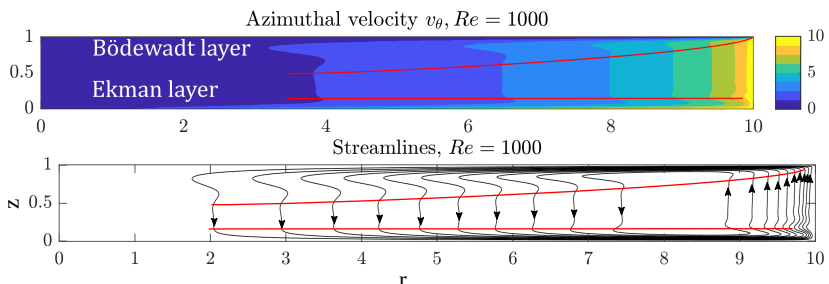


3D boundary layer/
cross flow instability

Navier-Stokes equations:

$$\begin{aligned}(\mathbf{U} \cdot \nabla) \mathbf{U} &= -\nabla P + \frac{1}{Re} \nabla^2 \mathbf{U} \\ \nabla \cdot \mathbf{U} &= 0\end{aligned}$$

solved with Finite Volume Method.
Dimensions: $(L, T, V) = (H, \frac{1}{\Omega}, H\Omega)$.
Solved with Newton method.



Bifurcation scenario - Linear Stability

Navier-Stokes equations linearised around the base flow \mathbf{U} :

$$\begin{aligned} \frac{\partial \mathbf{u}}{\partial t} + (\mathbf{u} \cdot \nabla) \mathbf{U} + (\mathbf{U} \cdot \nabla) \mathbf{u} = \\ -\nabla p + \frac{1}{Re} \nabla^2 \mathbf{u}, \quad \nabla \cdot \mathbf{u} = 0 \end{aligned}$$

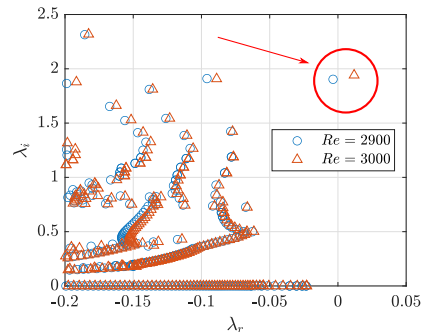
state vector $\mathbf{q} = [\mathbf{u}, p]$:

$$\mathbf{B} \frac{\partial \mathbf{q}}{\partial t} = \mathbf{A} \mathbf{q}$$

$$\mathbf{q} = \hat{\mathbf{q}} e^{\lambda t} + \hat{\mathbf{q}}^* e^{\lambda^* t}$$

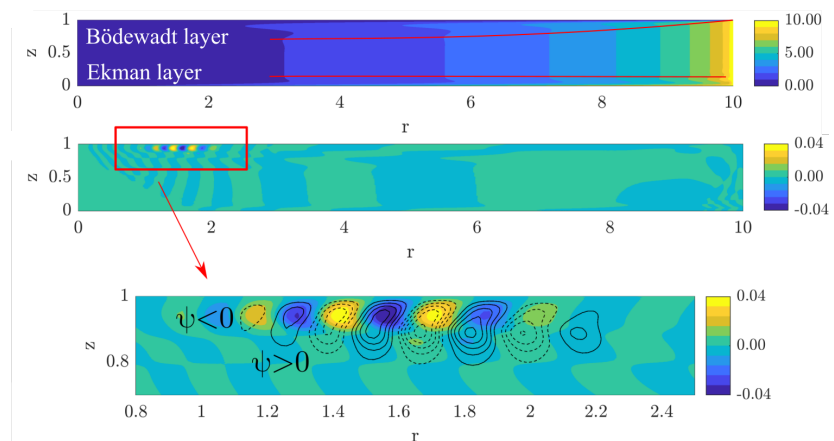
$$\lambda \mathbf{B} \hat{\mathbf{q}} = \mathbf{A} \hat{\mathbf{q}}$$

Solved with Arnoldi method
(ARPACK in the shift-invert mode).



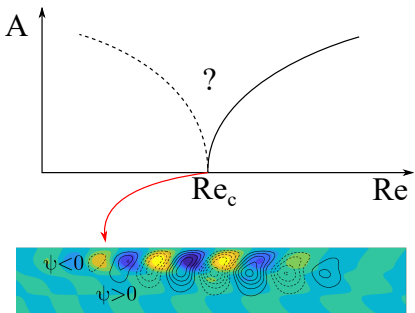
Instability at
 $Re_c = 2925.47$ (consistent
with Daube & Le Quéré
2001)

Bifurcation scenario - Linear Stability



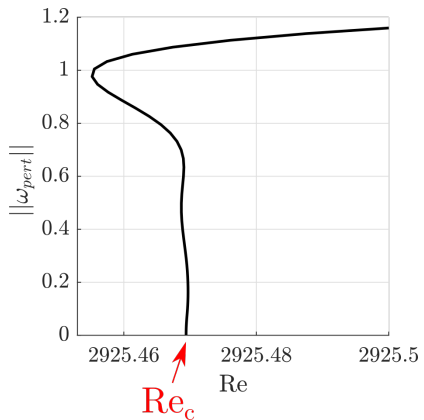
u_θ of the base flow and the most unstable eigenvector. Eigenvector consists of counter rotating rolls in the Bödewadt layer. $Re=3000$.

Bifurcation scenario - Harmonic Balance Method



Harmonic Balance Method , initial guess with Self-Consistent Method

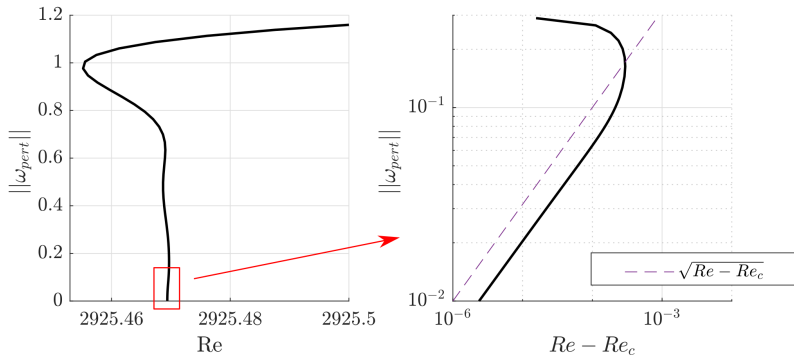
$$\mathbf{q} = \sum_{k=-N}^N \hat{\mathbf{q}}_k e^{ik\frac{2\pi}{T}t}$$



Azimuthal vorticity observable:

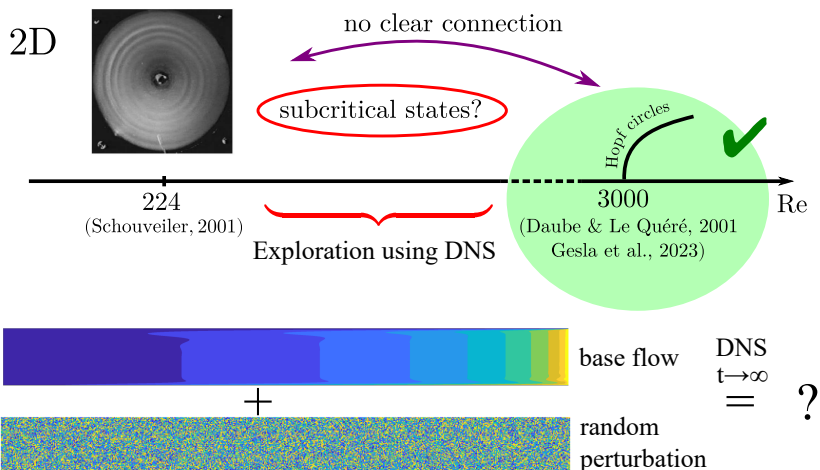
$$\|\omega_{pert}\| = \sqrt{\int |\omega - \omega_b|^2 r dr dz}$$

Bifurcation scenario - found branch



Branch emanating from the point of Hopf bifurcation ($Re=2925.47$) is supercritical, although in a tiny interval $\Delta Re/Re < 10^{-6}$.

Self-sustained scenario

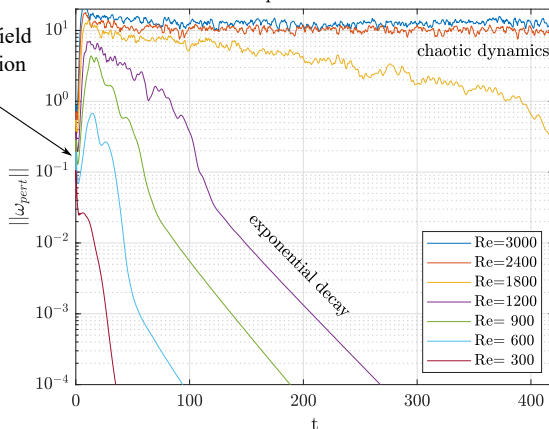


Systematic search

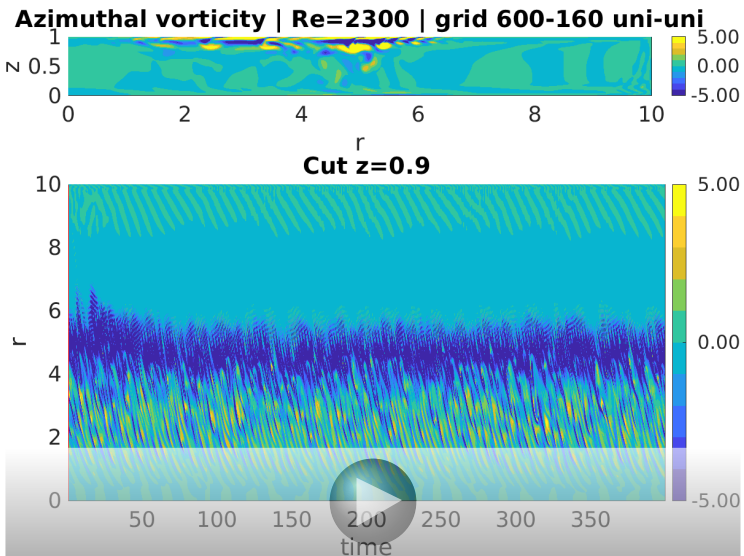
random field perturbation

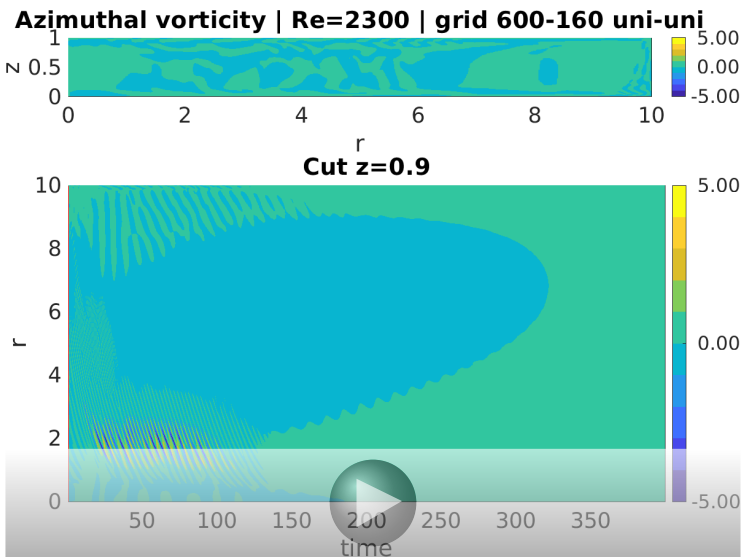
Asymptotic state depends on Re and perturbation amplitude.

Initial condition perturbed with random field

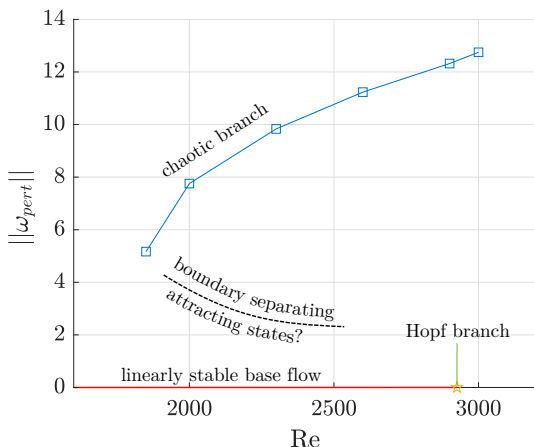


Chaotic self-sustained states are observed at $Re \gtrapprox 1800$.





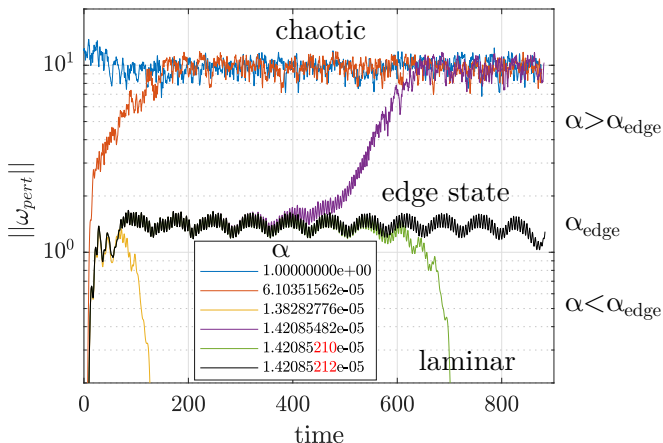
Chaotic branch



$1800 \gtrapprox Re < 3000$ two attracting states:

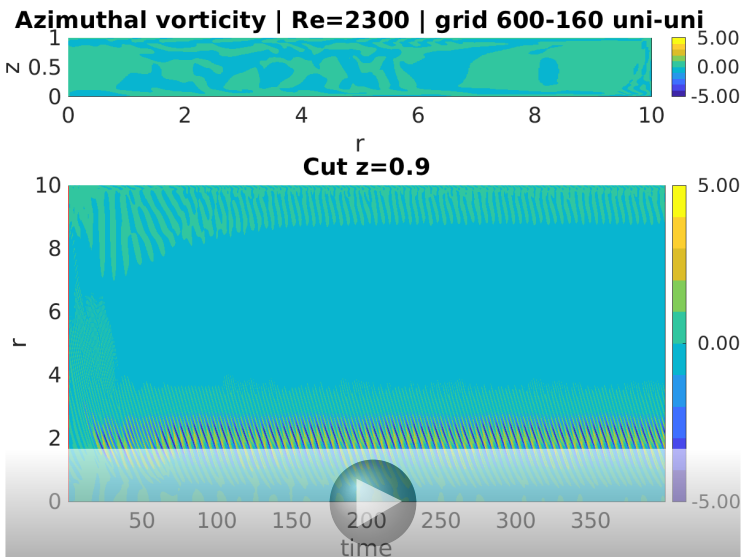
- base state
- chaotic state

are separated by a basin boundary, on which an *edge state* lies (Eckhardt *et al.*, 2007).

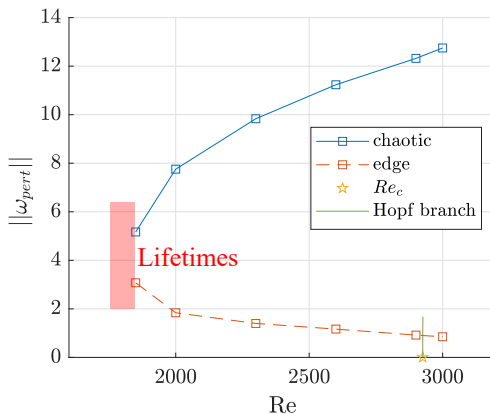
Edge state, $Re=2300$ 

Bisection procedure (e.g. Toh & Itano, JPSJ 2001):

$$u(t=0) = (1 - \alpha)u_{\text{laminar}} + \alpha u_{\text{chaotic}}, \quad 0 < \alpha < 1.$$

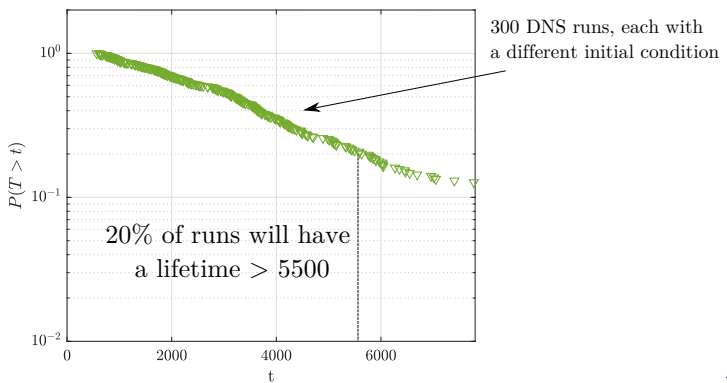
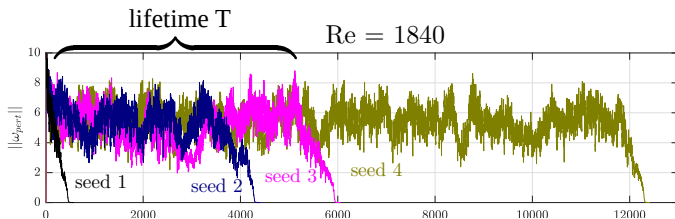


Self-sustained scenario - Summary

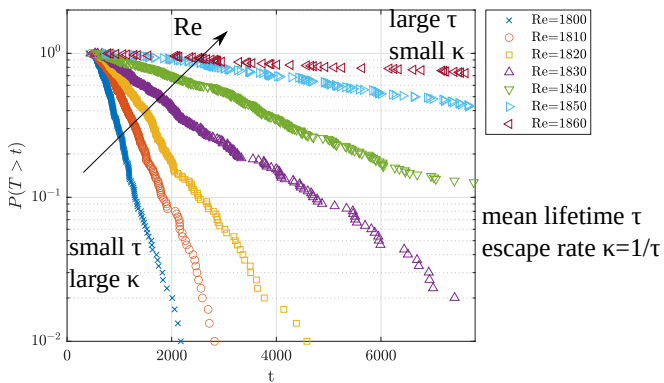
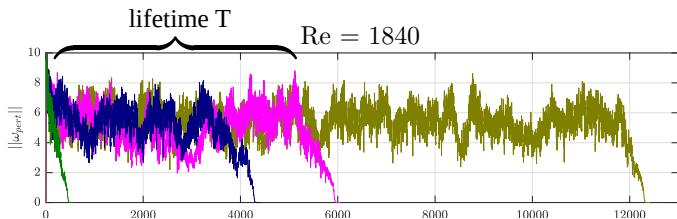


Subcritical solutions found for $Re > 1800$ complete the bifurcation diagram.

Lifetimes



Lifetimes

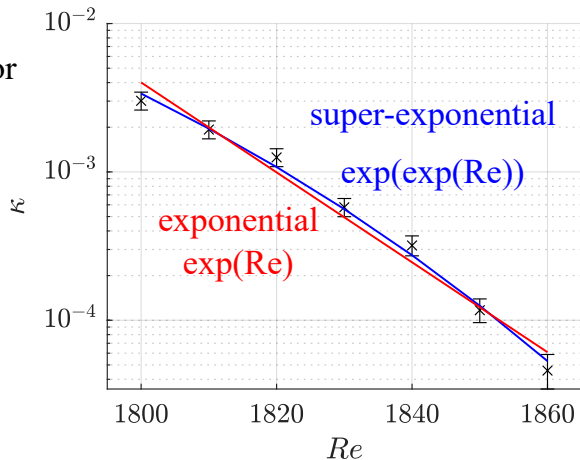


Lifetimes (methods: Avila *et al.*, 2010)

escape rate from
the leaky attractor

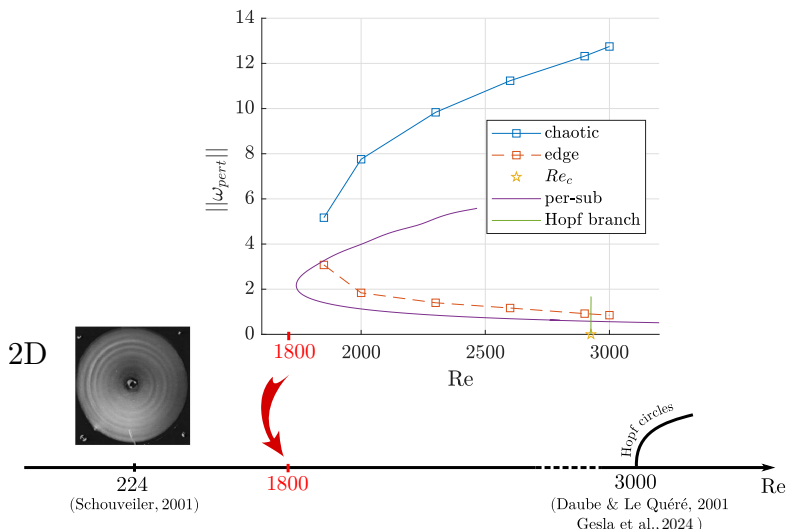
$$\kappa = 1/\tau$$

mean lifetime τ



Lifetime statistics follow a super-exponential law. Finite lifetimes can be observed only for $Re \in (1800, 1860)$.

Self-sustained scenario

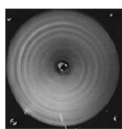


✗ Subcritical solutions do not explain the circular rolls observed experimentally. (Gesla et al., PRF 2024)

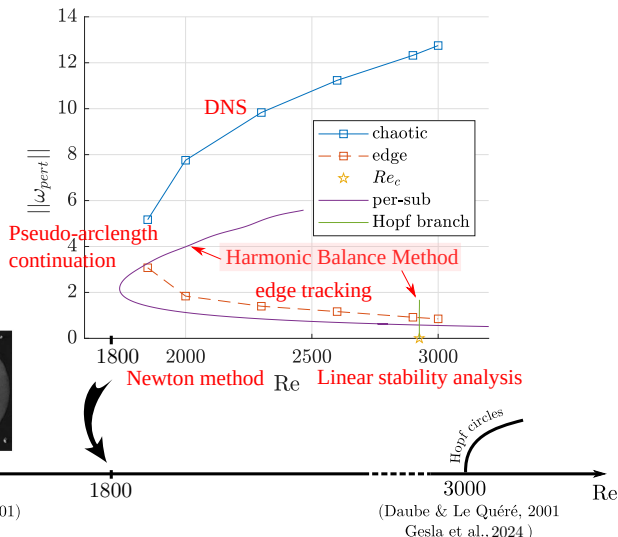
Methods

Methods:

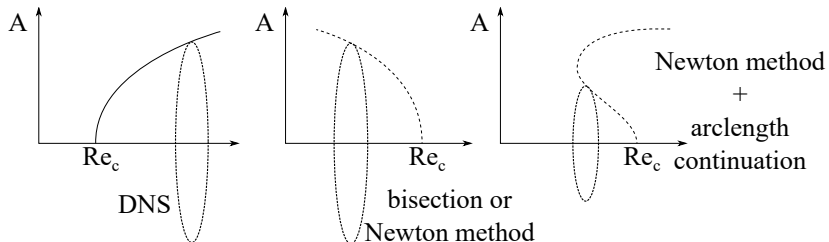
2D



224
(Schouwiler, 2001)



Harmonic Balance Method



HBM describes the time-periodic solutions in all the three cases above.

State vector

$$\mathbf{q}(\mathbf{x}, t) = [\mathbf{u}(\mathbf{x}, t), p(\mathbf{x}, t)]:$$

$$\mathbf{q}(\mathbf{x}, t) = \sum_{k=-N}^N \hat{\mathbf{q}}_k(\mathbf{x}) e^{ik\frac{2\pi}{T}t}.$$

Variables: $\hat{\mathbf{q}}_k(\mathbf{x})$ and T .

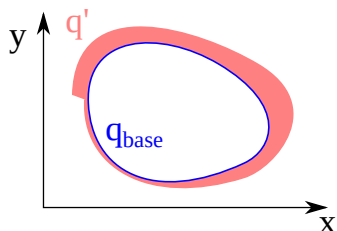
Equations:

$$\frac{\partial \mathbf{q}}{\partial t} = \mathcal{L}(\mathbf{q}) + \mathcal{N}(\mathbf{q}, \mathbf{q}),$$

phase condition (to find T), e.g.:

$$\frac{\partial \mathbf{q}}{\partial t}(\mathbf{x}_0, t_0) = 0.$$

Stability of the time periodic solution

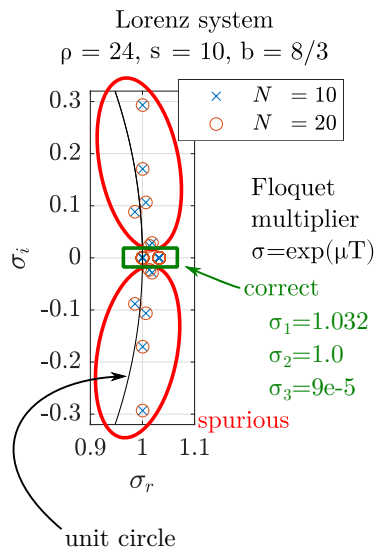


$$\mathbf{q} = \mathbf{q}_{\text{base}} + \mathbf{q}'$$

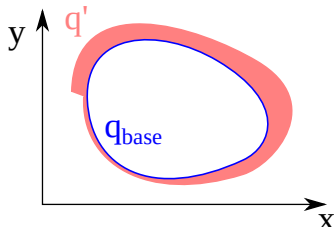
$$\text{HBM: } \mathbf{q}' = e^{\mu t} \sum_{k=-N}^N \hat{\mathbf{q}}'_k e^{ik\frac{2\pi}{T}t}$$

μ - Floquet exponent, determined modulo $i\frac{2\pi}{T}$

Lazarus, A. and Olivier T., A harmonic-based method for computing the stability of periodic solutions of dynamical systems (2010).



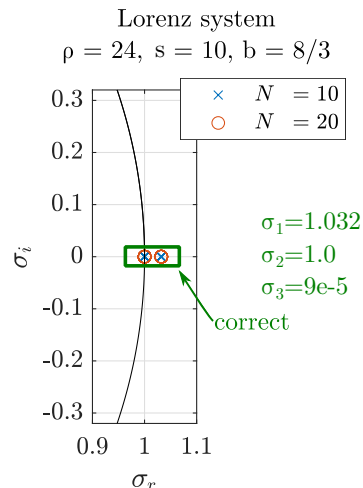
Stability of the time periodic solution



$$\mathbf{q} = \mathbf{q}_{base} + \mathbf{q}'$$

Chebyshev:

$$\mathbf{q}' = \sum_{k=0}^N \hat{\mathbf{q}}'_k T_k(2t/T - 1)$$



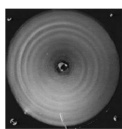
Gesla, A. et al., Stability analysis of periodic solutions in nonlinear dynamical systems using Chebyshev polynomial expansion, (under review in J. Sci. Comput.), 2024.

Self-sustained scenario

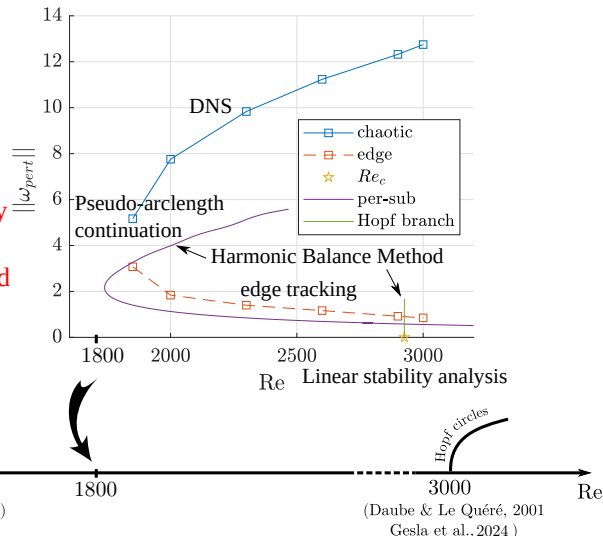
Methods:

Circular rolls
observed
experimentally
are not
a self-sustained
state.

2D



224
(Schouwiler, 2001)



Another approach

Gauthier *et al.* (1999) writes in the abstract:

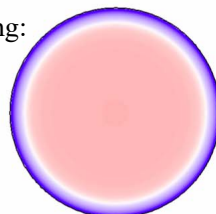
angular velocity. These structures occur naturally but can also be forced by small modulations of the angular velocity of the disk. For each rotation rate the dispersion

and in the core of the article:

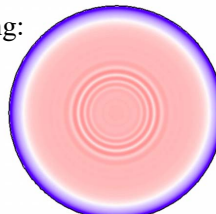
aggregate toward the centre and disappear at a given radius. Note that the threshold for the circle appearance depends on the noise level. With previous less regulated motors, the threshold was found to be $Re \approx 70$ while with the motors now used this threshold is found to be $Re \approx 110$. On increasing the angular velocity, the circles are more

Also Lopez *et al.* (2009) observe the rolls when forcing is applied:

No forcing:



Forcing:



Noise-sustained regime

1 Introduction

- Motivation
- Flow configuration

2 Self-sustained regime

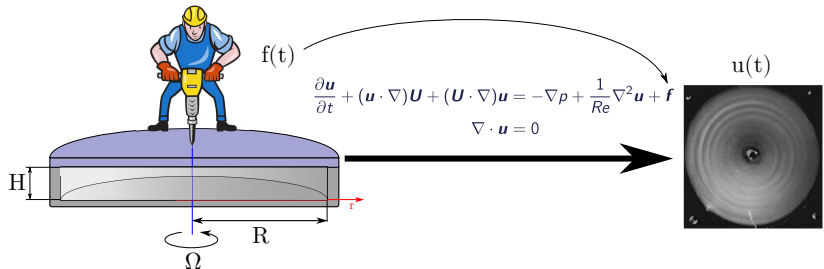
- Linear stability and Hopf branch
- Large amplitude chaotic branch and edge state

3 Noise-sustained regime

- Optimal forcing through resolvent analysis
- Noise response and comparison with experiments

4 Summary and outlooks

Origin of circular rolls – noise-sustained scenario



Assume that the forcing \mathbf{f} and the response \mathbf{u} are periodic:

$$\mathbf{f}(t) = \hat{\mathbf{f}} e^{i\omega t}, \quad \mathbf{u}(t) = \hat{\mathbf{u}} e^{i\omega t}$$

Forced equations linearised around the base flow:

$$\dot{\mathbf{u}} = \mathbf{A}\mathbf{u} + \mathbf{f}$$

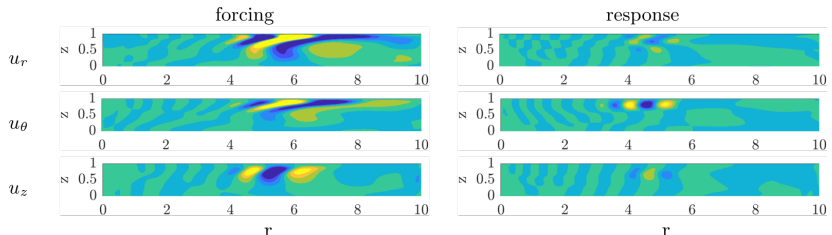
Linear relation (resolvent) between $\hat{\mathbf{f}}$ and $\hat{\mathbf{u}}$:

$$\mathbf{R}(\omega) \hat{\mathbf{f}} = \hat{\mathbf{u}}, \quad \mathbf{R}(\omega) = (i\omega \mathbf{I} - \mathbf{A})^{-1}$$

Optimal forcing and response | Resolvent (Trefethen & Embree, 2005)

Optimal gain G is the largest singular value¹ of
 $\mathbf{R}(\omega) = (i\omega \mathbf{I} - \mathbf{A})^{-1}$.

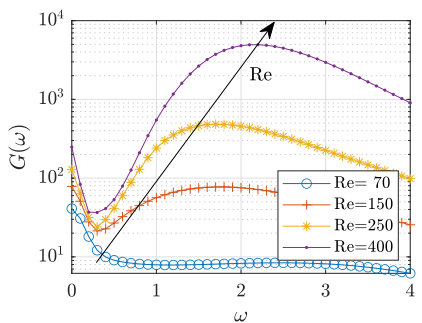
$$G = \frac{\text{"strength" of } \mathbf{u}}{\text{"strength" of } \mathbf{f}} = \frac{||\hat{\mathbf{u}}(r, z)||^2}{||\hat{\mathbf{f}}(r, z)||^2}$$



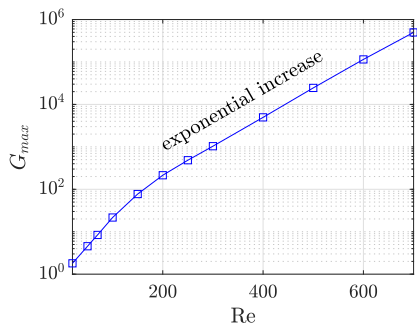
Real part of perturbation velocity for the optimal forcing and response at $\omega = 1.7$ and $\text{Re}=250$. Fields normalised with $||\hat{\mathbf{u}}|| = ||\hat{\mathbf{f}}|| = 1$.

¹ methodology in Cerqueira & Sipp (2014)

Optimal gain G



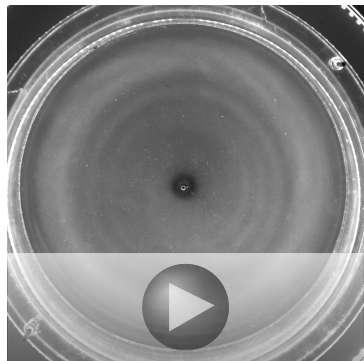
Optimal gain $G(\omega)$



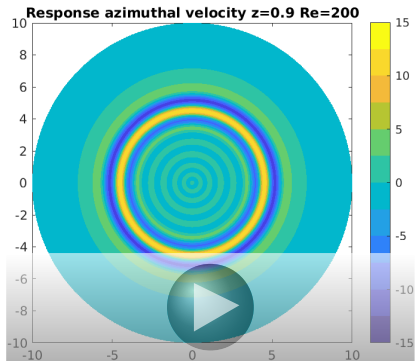
Maximal G over $\omega > 1$

- **optimal response** has a form of rolls in Bödewadt layer
- **strong optimal gain:** $G=200$ at $Re=200$, exponential dependence in Re
- nonnormal effect may be **wrongly interpreted** as a linear instability in the experimental set-up

Visualisation



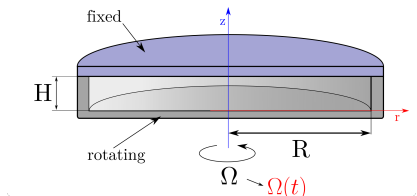
Circular rolls, $Re=205$ [F. Bruno]



Optimal response, $Re=200$

Is this mechanism relevant for the experiments?

Boundary forcing (Lopez *et al.*, PoF 2009, Do *et al.*, PRE 2010)



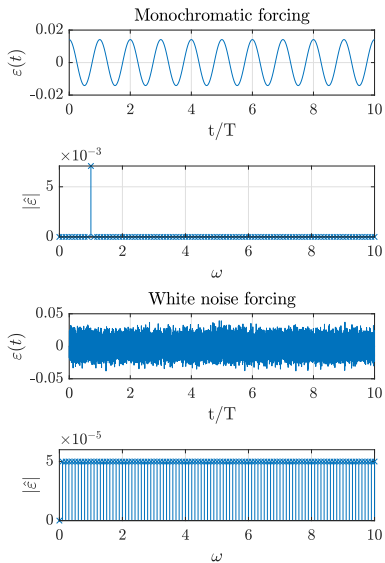
$$\Omega(t) = \Omega_0(1 + \varepsilon(t))$$

$\varepsilon(t)$ can be for example:

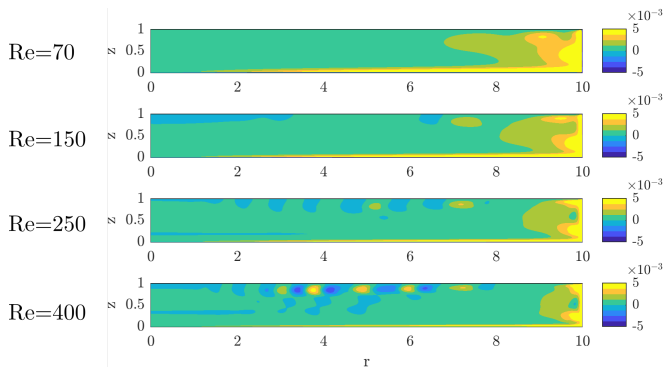
- monochromatic
- Gaussian white noise

Normalisation: $rmse(\varepsilon(t)) = 0.01$

Tool: time integration



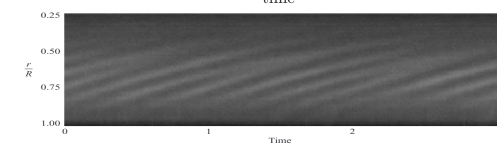
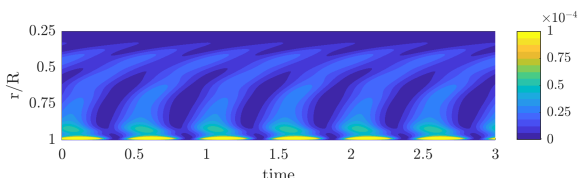
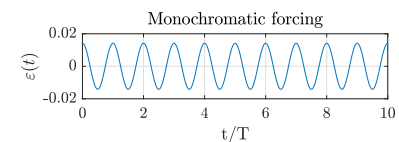
Boundary white noise forcing of finite amplitude



Snapshots of $u_\theta(r, z)$ in the presence of white noise forcing.

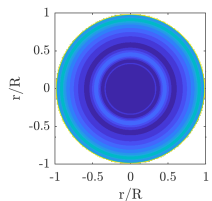
Response to the boundary forcing still features rolls.

Experimental comparison against Schouveiler et al., 2001 ($R/H=8.75$)

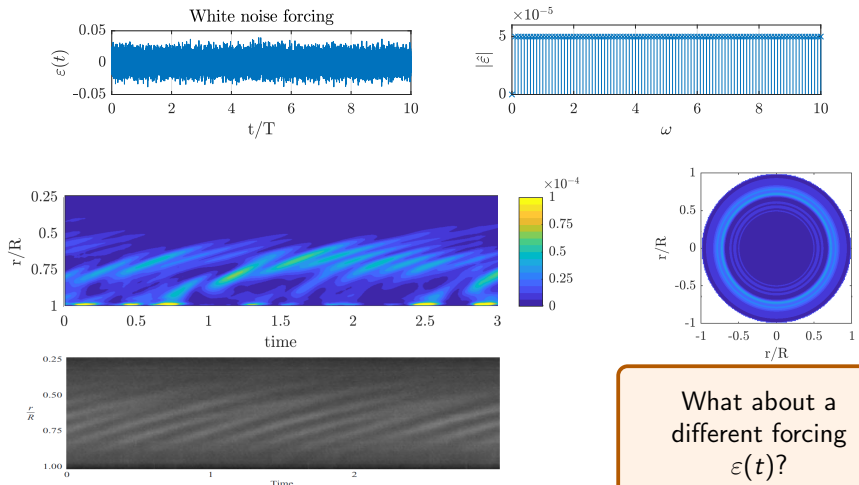


Energy observable $E(r, t)$:

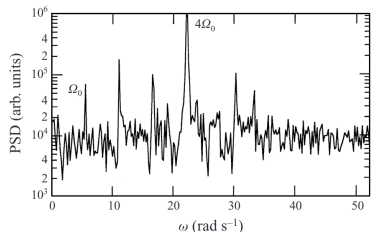
$$\int_{0.2}^1 ((u_r)^2 + (u_\theta)^2 + (u_z)^2) dz$$



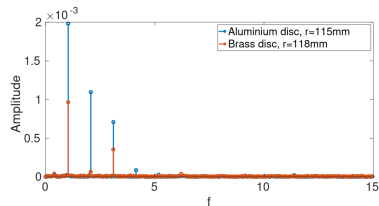
Experiment:
periodic response
and roll pairing.

Experimental comparison against Schouveiler et al., 2001 ($R/H=8.75$)

Harmonic forcing

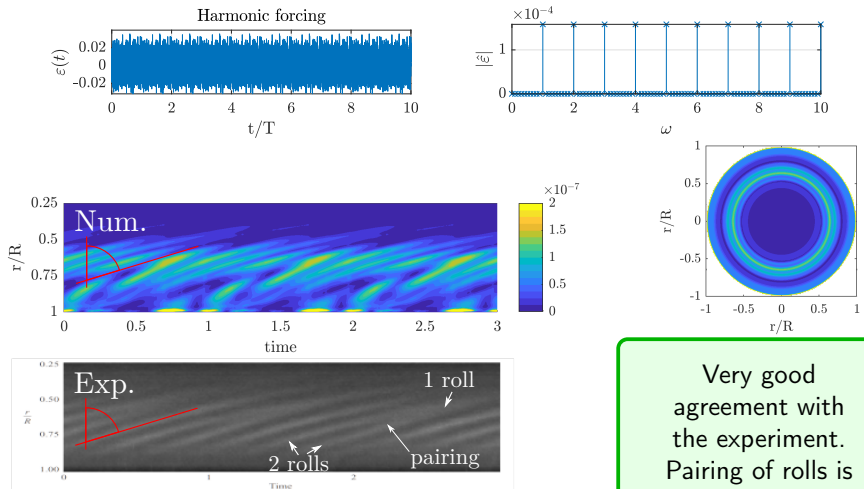


Spectrum of circular rolls signal with no external forcing applied. Disc angular frequency Ω_0 . $\text{Re}=128$.
 $\text{R/H}=20.9$. [Gauthier et al., 1999]



Spectrum of the disc's surface vertical displacement.
[Faugaret, 2021]

Perturbation in the experiment involves mainly the harmonics of the disc's angular frequency.

Experimental comparison against Schouveiler et al., 2001 ($R/H=8.75$)

Very good agreement with the experiment. Pairing of rolls is also captured.

Summary and outlooks

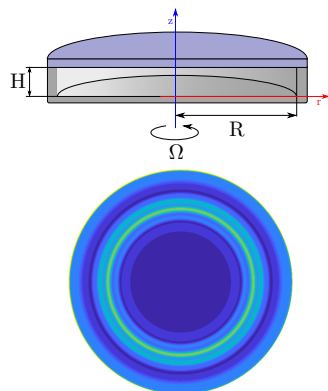
Summary

Explored scenarios:

- self-sustained scenario (periodic and chaotic solutions)
- noise-sustained scenario (optimal and boundary forcing)

Developed tools (C++ and MATLAB):

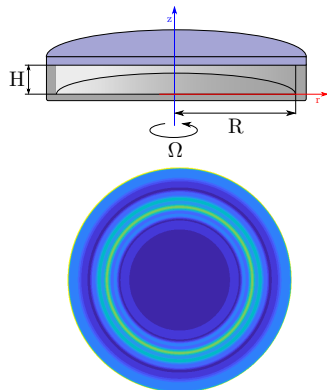
- Newton method (base flow) + Arnoldi/ARPACK (stability)
- axisymmetric time integration (nonlin./lin.)
- periodic solutions (HBM, SCM, Chebyshev)
- optimal forcing (SVD of the resolvent)



Summary

Circular rolls (at $Re \approx 200$):

- ✗ not an instability mode
- ✗ not a subcritical solution
- ✓ response to external forcing
 - optimal gain $G > 100$
(resolvent analysis)
 - result of boundary forcing
(time integration)
 - response to the forcing is linear



Subcritical axisymmetric solutions in rotor-stator flow, Gesla et al., Phys. Rev. Fluids 9, 2024.

On the origin of circular rolls in rotor-stator flow, Gesla et al., J. Fluid Mech. 1000:A47.

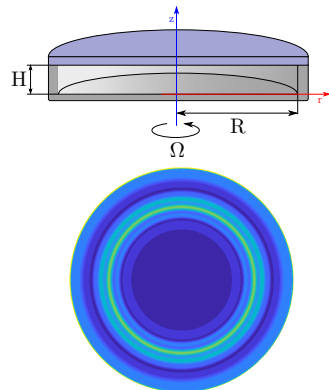
Stability analysis of periodic solutions in nonlinear dynamical systems using Chebyshev polynomial expansion, Gesla et al., under review in J. Sci. Comput., 2024.

From annular cavity to rotor-stator flow: nonlinear dynamics of axisymmetric rolls, Gesla et al., to be submitted to Phys. Rev. Fluids, 2024.

Summary and outlooks

Outlooks:

- interaction of spiral and circular rolls (DNS: Xie *et al.*, JFM 2024; harmonic resolvent)
- effect of the aspect ratio, configurations with a hub
- sensitivity through an adjoint analysis
- experimental confirmation of the forcing gain and response



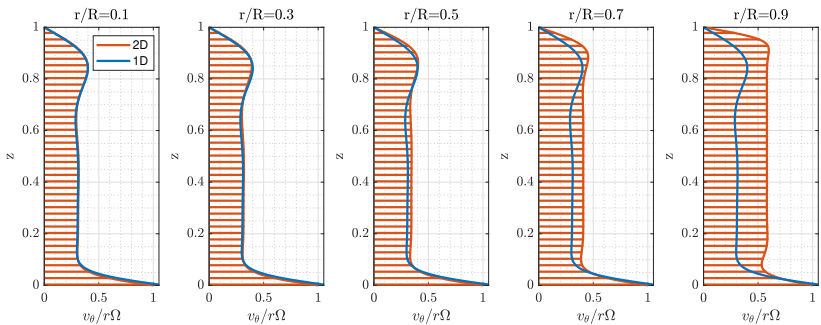
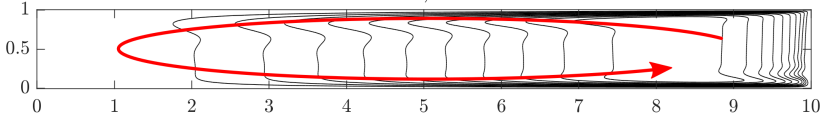
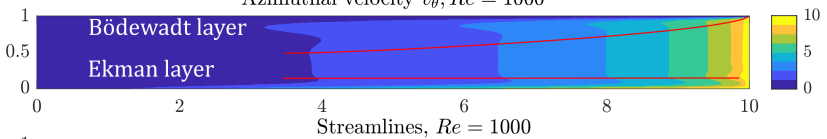
Subcritical axisymmetric solutions in rotor-stator flow, Gesla *et al.*, Phys. Rev. Fluids 9, 2024.

On the origin of circular rolls in rotor-stator flow, Gesla *et al.*, J. Fluid Mech. 1000:A47.

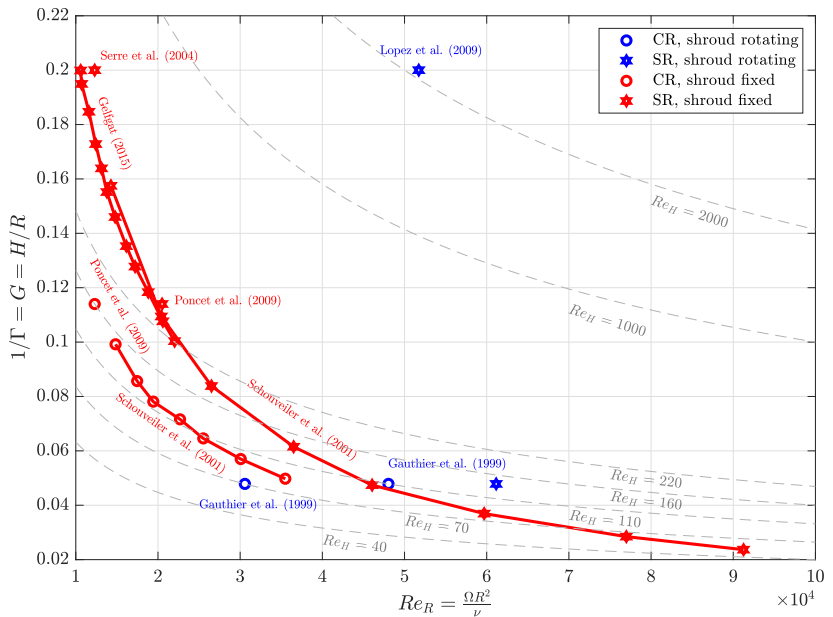
Stability analysis of periodic solutions in nonlinear dynamical systems using Chebyshev polynomial expansion, Gesla *et al.*, under review in J. Sci. Comput., 2024.

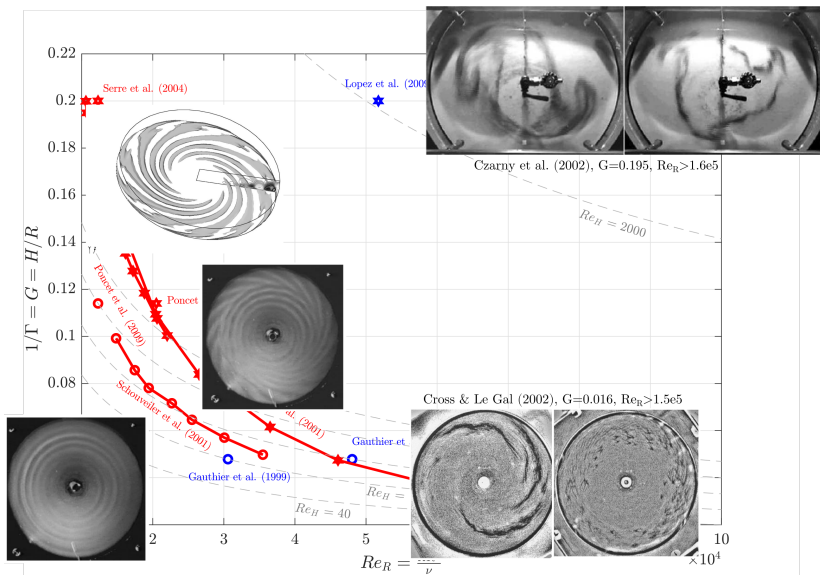
From annular cavity to rotor-stator flow: nonlinear dynamics of axisymmetric rolls, Gesla *et al.*, to be submitted to Phys. Rev. Fluids, 2024.

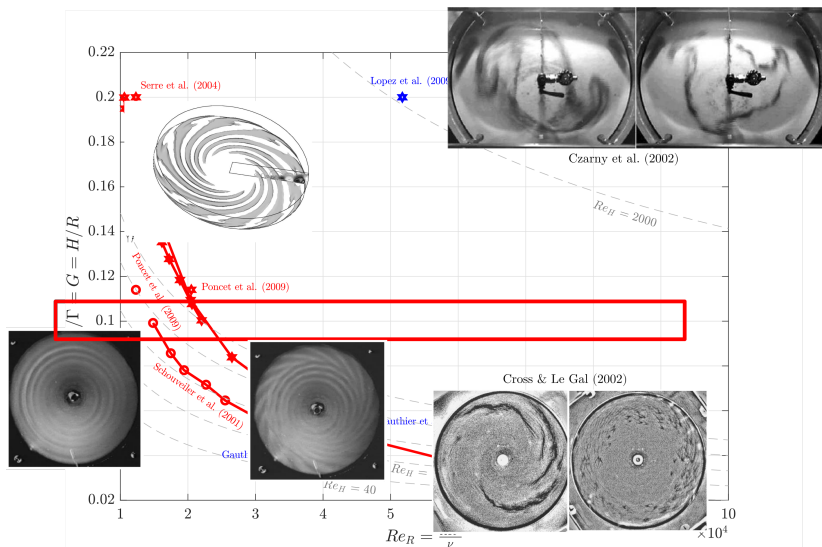
2D Base flow

Azimuthal velocity $v_\theta, Re = 1000$ 

Literature overview, shallow cavities $H/R < 0.2$



Literature overview, shallow cavities $H/R < 0.2$ 

Focus of current work, $H/R=0.1$ 

Finding the optimal forcing

Navier-Stokes equations:

$$\begin{cases} \frac{\partial \mathbf{u}}{\partial t} + (\mathbf{u} \cdot \nabla) \mathbf{u} = -\nabla p \\ + \frac{1}{Re} \nabla^2 \mathbf{u} + \mathbf{f}, \quad \nabla \cdot \mathbf{u} = 0 \end{cases}$$

Linearised around \mathbf{U} :

$$\begin{cases} \frac{\partial \mathbf{u}}{\partial t} + (\mathbf{u} \cdot \nabla) \mathbf{U} + (\mathbf{U} \cdot \nabla) \mathbf{u} = \\ -\nabla p + \frac{1}{Re} \nabla^2 \mathbf{u} + \mathbf{f}, \quad \nabla \cdot \mathbf{u} = 0 \end{cases}$$

$\mathbf{q} = [\mathbf{u}, p]$, Finite Volume Method

$$\mathbf{B} \frac{\partial \mathbf{q}}{\partial t} = \mathbf{Aq} + \mathbf{f}$$

$$\mathbf{q} = \hat{\mathbf{q}} e^{i\omega t} + \hat{\mathbf{q}}^* e^{-i\omega t}$$

$$(i\omega \mathbf{B} - \mathbf{A}) \hat{\mathbf{q}} = \hat{\mathbf{f}}$$

$$\underbrace{\mathbf{P}^* (i\omega \mathbf{B} - \mathbf{A}) \mathbf{P}}_{\mathbf{R}^{-1}} \hat{\mathbf{u}} = \hat{\mathbf{f}}, \quad \mathbf{P} \hat{\mathbf{u}} = \hat{\mathbf{q}}$$

Resolvent \mathbf{R} :

$$\mathbf{R} = \mathbf{P}^* (i\omega \mathbf{B} - \mathbf{A})^{-1} \mathbf{P}$$

Singular Value Decomposition of \mathbf{R} will yield an optimal forcing.

Prolongation

Prolongation matrix P

$$Pu = q$$

P - rectangular matrix

$$\begin{bmatrix} 0 & 0 & 0 & \dots \\ 1 & 0 & 0 & \dots \\ 0 & 1 & 0 & \dots \\ 0 & 0 & 1 & \dots \\ \vdots & \vdots & \vdots & \ddots \end{bmatrix} \begin{bmatrix} u \\ v \\ w \\ \vdots \end{bmatrix} = \begin{bmatrix} 0 \\ u \\ v \\ w \\ \vdots \end{bmatrix}$$

Singular Value Decomposition

$$\hat{u} = R\hat{f}$$

U, V - unitary matrices
(columns are orthogonal)

$$\hat{u} = U\Sigma V^* \hat{f}$$

* - conjugate transpose

$$\begin{bmatrix} \hat{u}_1 \\ \vdots \\ \hat{u}_n \end{bmatrix} = \underbrace{\left(\begin{bmatrix} u_{11} \\ \vdots \\ u_{n1} \end{bmatrix} \dots \begin{bmatrix} u_{1n} \\ \vdots \\ u_{nn} \end{bmatrix} \right)}_U \underbrace{\begin{pmatrix} \sigma_1 & \dots & 0 \\ \vdots & \ddots & \vdots \\ 0 & \dots & \sigma_n \end{pmatrix}}_\Sigma \underbrace{\left(\begin{bmatrix} v_{11} & \dots & v_{1n} \\ \vdots & \ddots & \vdots \\ [v_{n1} & \dots & v_{nn}] \end{bmatrix}\right)}_{V^*} \begin{bmatrix} \hat{f}_1 \\ \vdots \\ \hat{f}_n \end{bmatrix}$$

U - orthogonal basis of responses

V - orthogonal basis of forcings

Strongest response - largest σ

Equivalent eigenvalue problem

$\hat{\mathbf{u}} = \mathbf{R}\hat{\mathbf{f}}$ can be transformed:

$$\mathbf{R}^* \mathbf{R} \hat{\mathbf{f}} = \sigma^2 \hat{\mathbf{f}}$$

in polar coordinates:

$$\underbrace{\mathbf{R}^* \mathbf{Q} \mathbf{R}}_{\mathbf{A}} \underbrace{\hat{\mathbf{f}}}_{\mathbf{v}} = \underbrace{\sigma^2}_{\lambda} \underbrace{\mathbf{Q}}_{\mathbf{B}} \underbrace{\hat{\mathbf{f}}}_{\mathbf{v}}$$

Eigenvalue problem $\mathbf{Av} = \lambda \mathbf{Bv}$
can be solved in MATLAB.

Hermitian eigenvalue
problem $\rightarrow \lambda = \sigma^2 \in \mathbb{R}$.

Double kinetic energy:

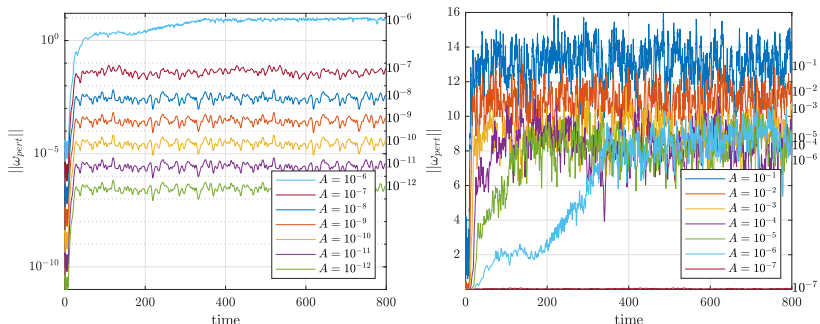
$$\mathbf{u}^* \mathbf{Qu} = \int_{\Omega} u_r^2 + u_\theta^2 + u_z^2 \ r dr dz$$

\mathbf{Q} expresses the cell volume:

$$\mathbf{Q} = \begin{bmatrix} r dr dz & \dots & 0 \\ \vdots & \ddots & \vdots \\ 0 & \dots & r dr dz \end{bmatrix}$$

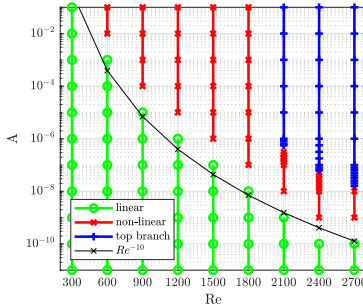
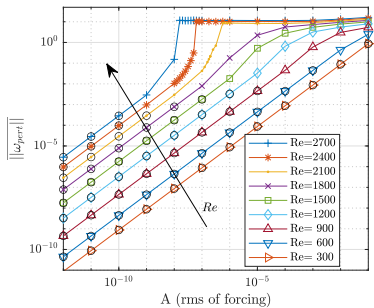
Linearity

White noise forcing: $\Omega(t) = \Omega_0(1 + A\varepsilon(t))$, $\text{rms}(\varepsilon(t))=1$



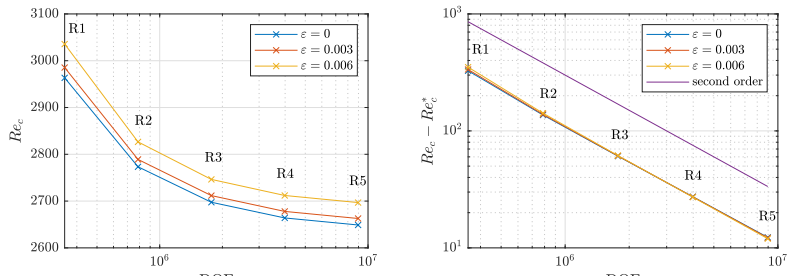
Vorticity observable depending on the forcing amplitude A . $\text{Re}=2100$.
Response is linear for $A < 10^{-8}$

Linearity



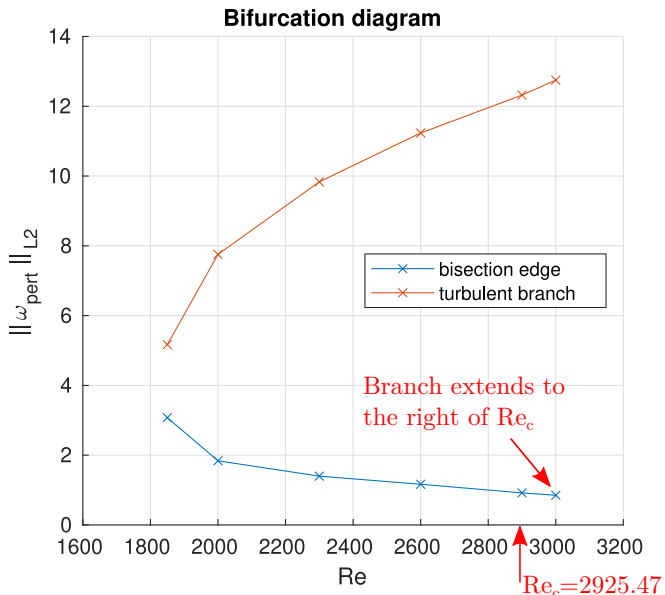
Response is linear for $Re < 300$. Circular rolls are therefore a linear response to the forcing.

Re_c mesh convergence



resolution	N_r	N_z	type	DOF	$\varepsilon = 0$	$\varepsilon = 0.003$	$\varepsilon = 0.006$
R0	600	160	uniform	390 k	2925.47		
R1	683	128	non-uniform	356 k	2963.41	2985.43	3035.61
R2	1024	192	non-uniform	796 k	2773.3	2789.01	2826.55
R3	1536	288	non-uniform	1.7 m	2697.48	2711.71	2746.33
R4	2304	432	non-uniform	4.0 m	2663.96	2677.9	2711.97
R5	3456	648	non-uniform	9.0 m	2648.9	2662.8	2696.8
				extrapolation	2636.61	2650.59	2684.81
				order	2.01	2.04	2.09

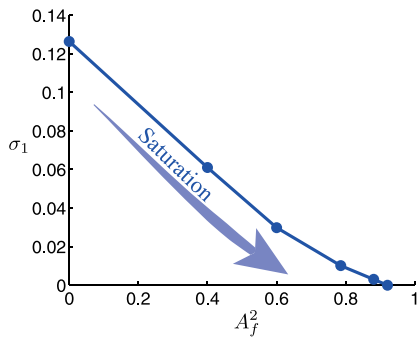
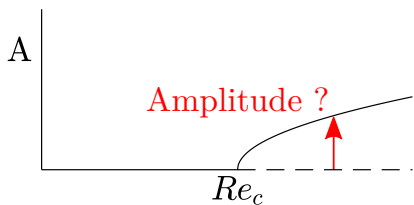
TABLE V. Critical Reynolds number Re_c depending on the the spatial discretisation. From R1 to R5 the ratio between two consecutive grid resolutions is 1.5 in each direction.



→ Find the branch bifurcating at Re_c

Finding the branch bifurcating at Re_c

If it was a supercritical bifurcation:



Mantic-Lugo et al., PRL 2014

- ✓ Self Consistent Method (SCM) (Mantic-Lugo et al., PRL 2014) gives approximately amplitude of the limit cycle
- ➡ use the SCM to find the branch

Self Consistent Method

- force the NS equations with the Reynolds stress term:
 $2A^2(\hat{u}' \cdot \nabla)u'$
- iterate on A to get a neutrally stable field U

Assumption:

$$u = U + u'e^{\lambda t} + \hat{u}'e^{\hat{\lambda}t}$$

and iteratively solve the following:

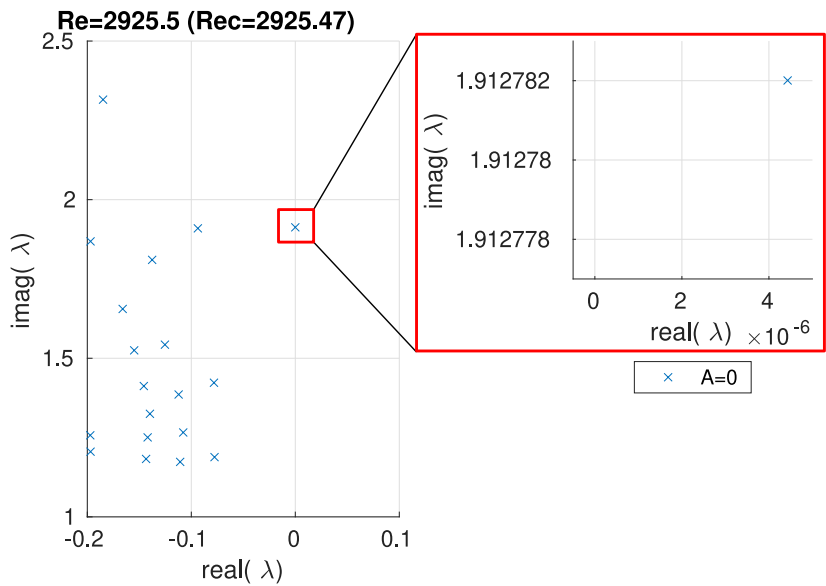
1) Forced NS equation:

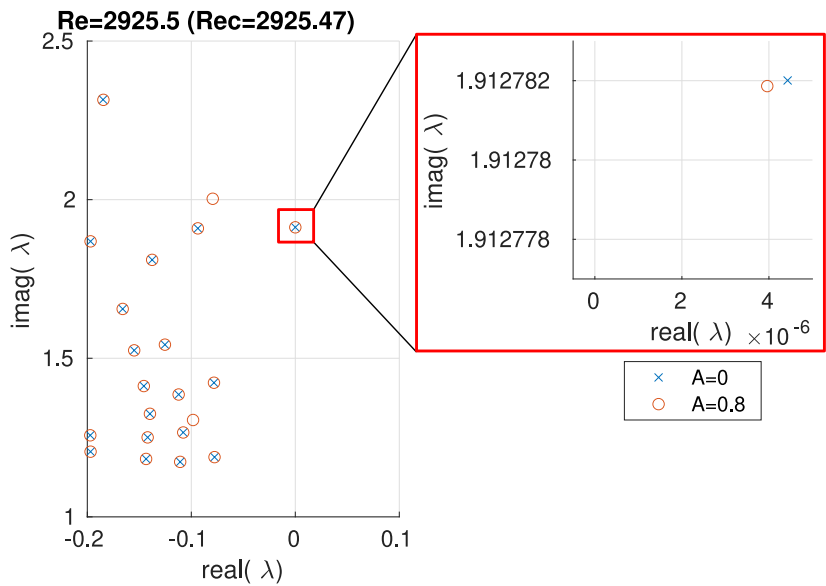
$$(U \cdot \nabla)U + 2A^2(\hat{u}' \cdot \nabla)u' = -\frac{1}{\rho}\nabla P + \frac{1}{Re}\Delta U$$

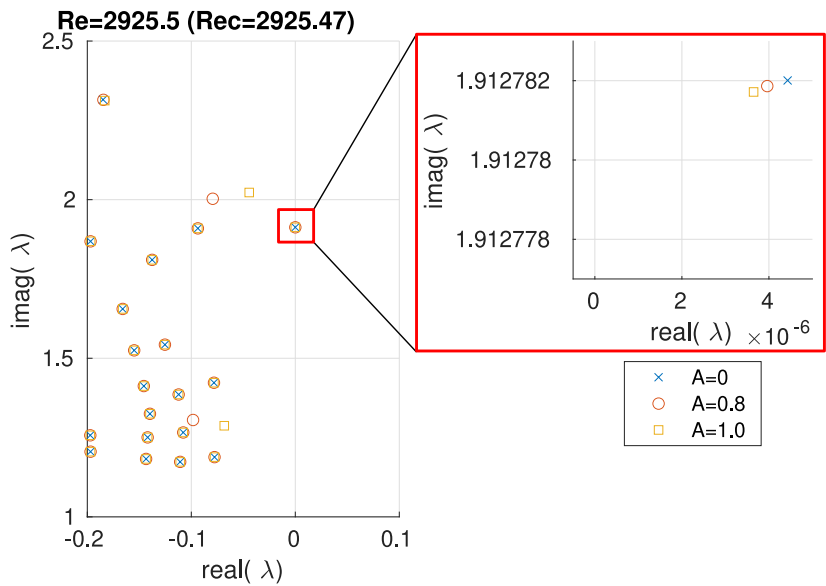
2) Eigenvalue problem:

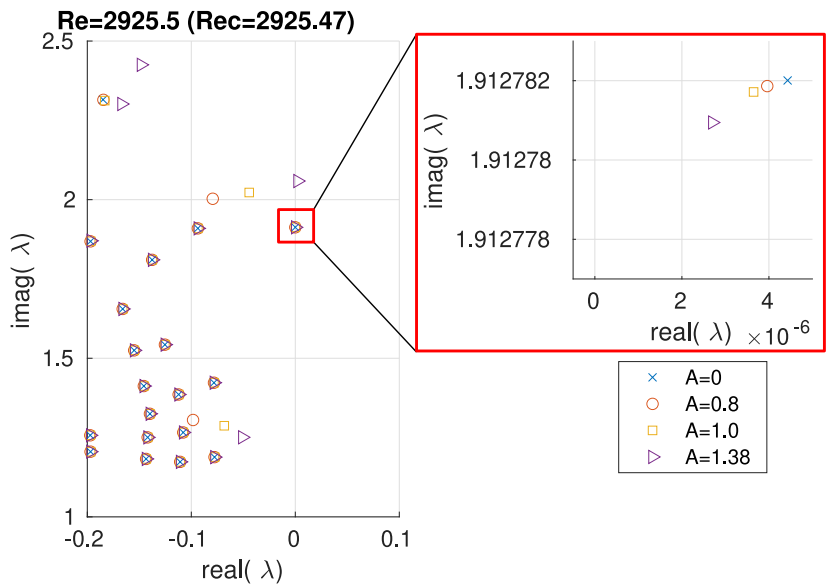
$$\lambda u' + (u' \cdot \nabla)U + (U \cdot \nabla)u' = -\frac{1}{\rho}\nabla p' + \frac{1}{Re}\Delta u'$$

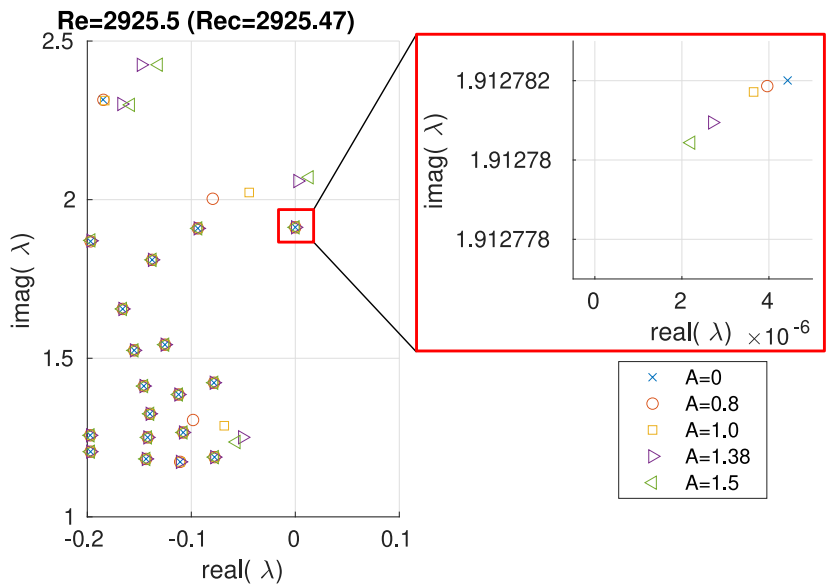
→ Find A such that U is neutrally stable, i.e. $\text{real}(\lambda)=0$

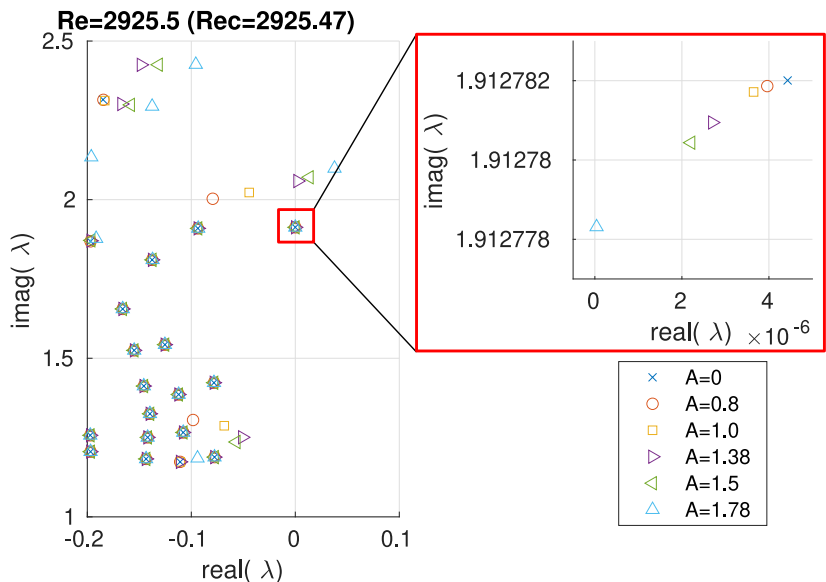


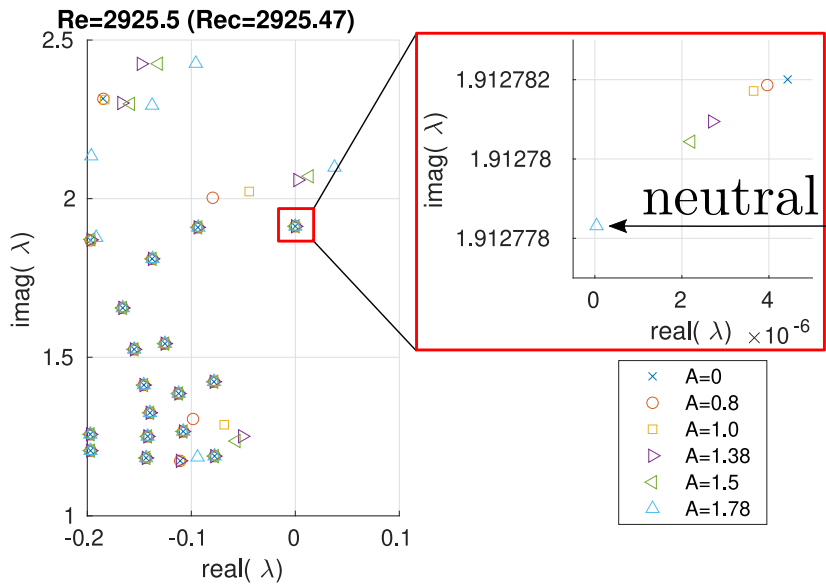




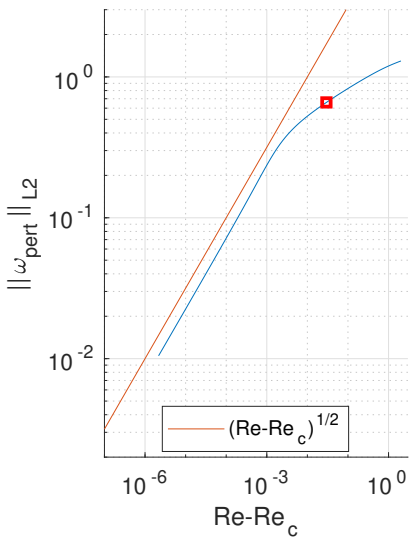
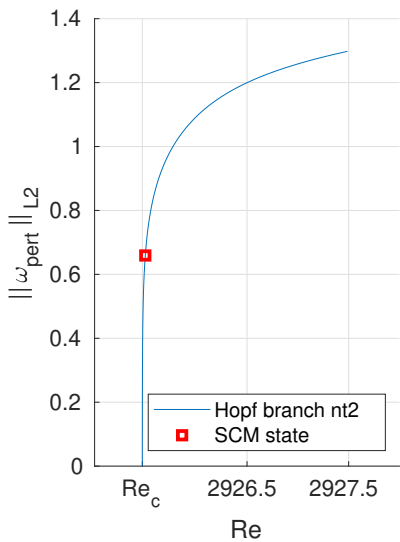








Bifurcation diagram



SCM is equivalent to expressing the limit cycle with one Fourier mode (also in Bengana & Tuckerman, PRF 2021).

$$nt = 2 : \quad u = U + u' e^{i\omega t} + \hat{u}' e^{-i\omega t}$$

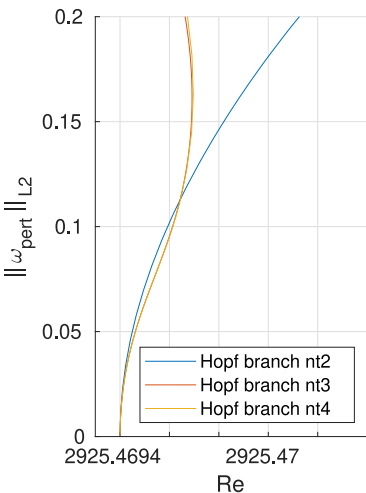
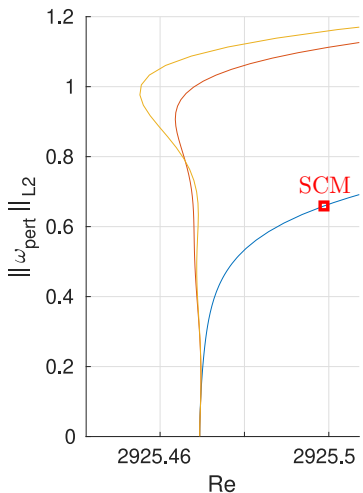
If more modes are added:

$$nt = 3, 4, \dots : \quad u = U + \sum_{k=1}^{nt} u^k e^{ik\omega t} + \hat{u}^k e^{-ik\omega t}$$

This can be substituted into NS equations and solved with Newton method:

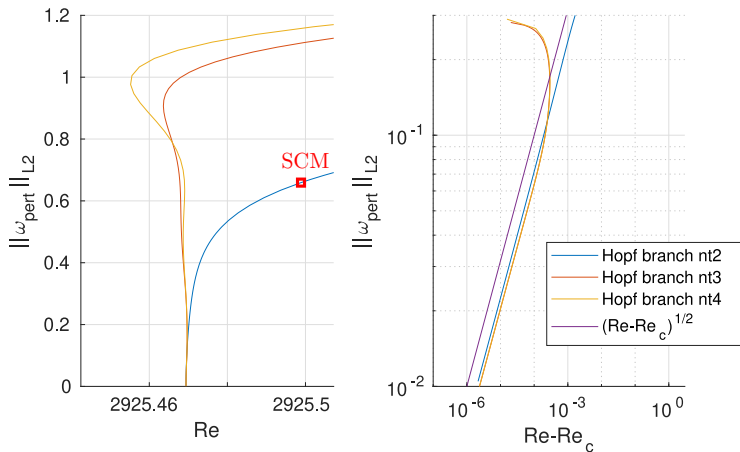
- ➡ SCM forms the initial guess for the Newton method
- ➡ Arclength continuation to get the branch

Bifurcation diagram

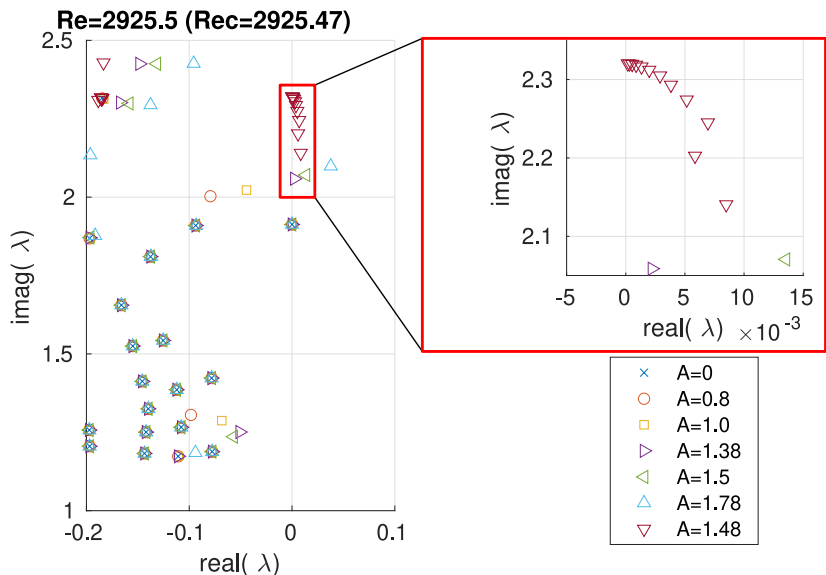


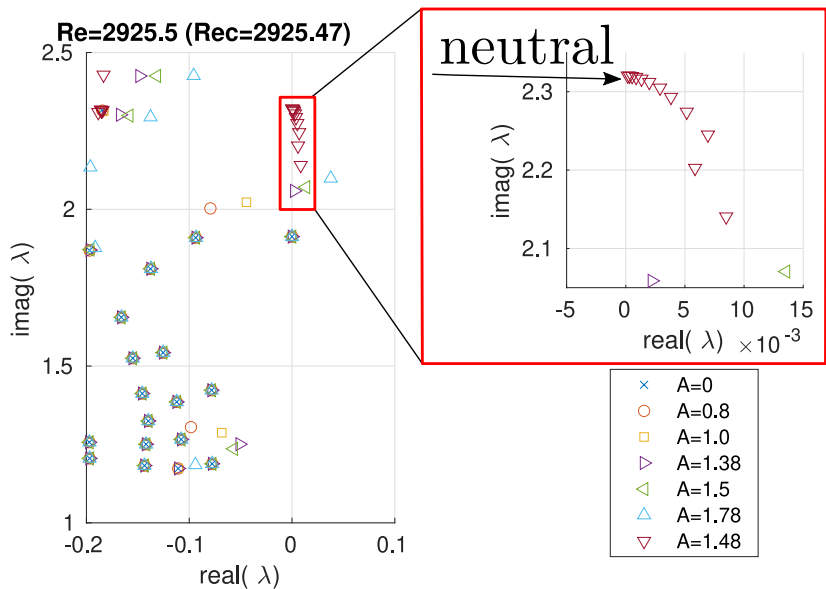
👉 supercritical Hopf bifurcation

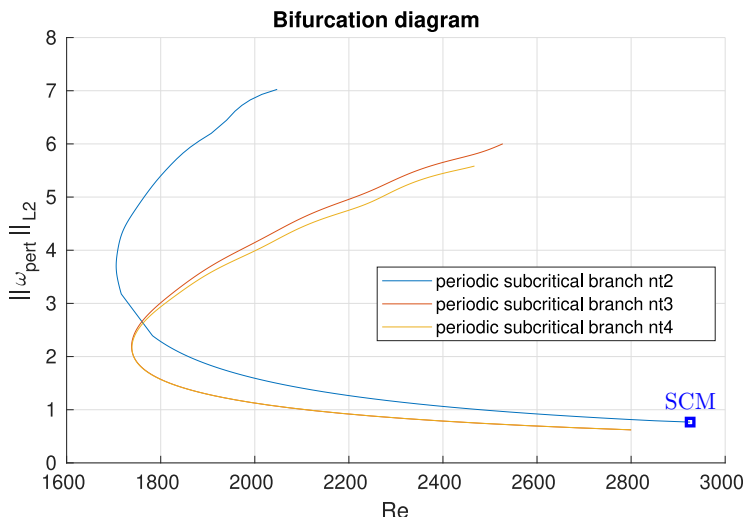
Bifurcation diagram

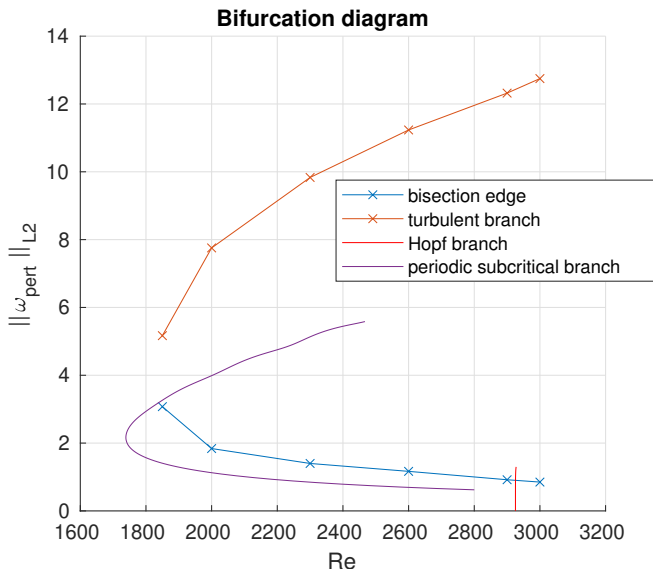


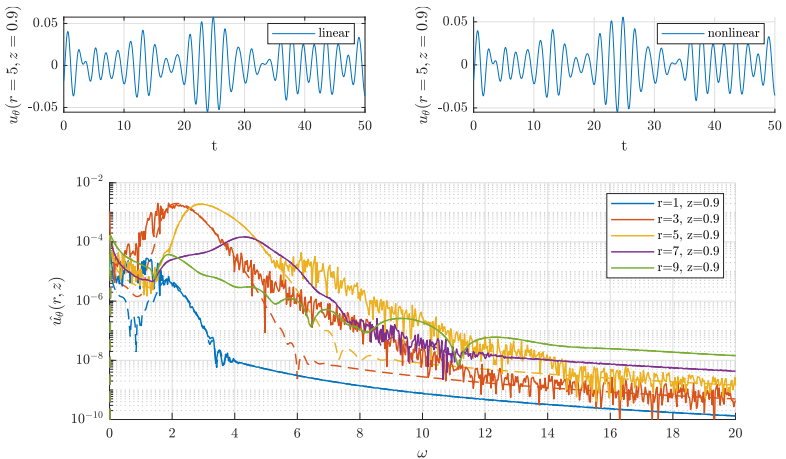
- 👉 supercritical Hopf bifurcation
- 👉 square root scaling only up to 10^{-4} from Re_c
- 👉 first fold at $5 \cdot 10^{-4}$ from Re_c



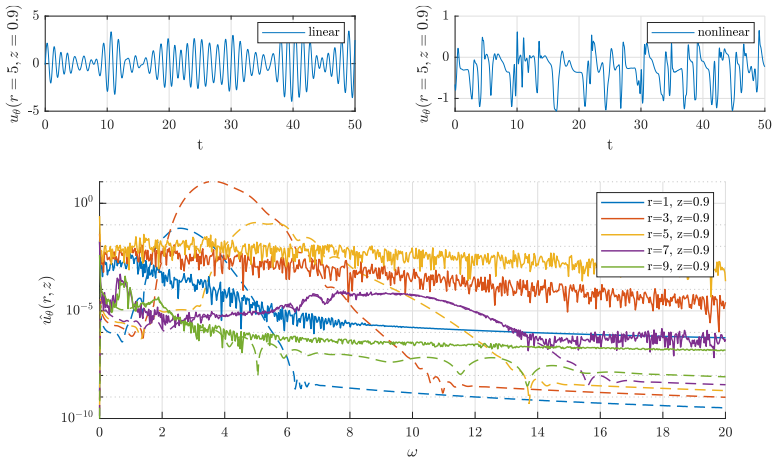




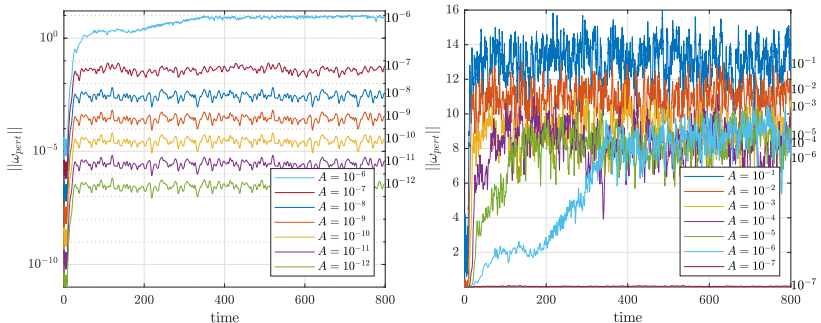




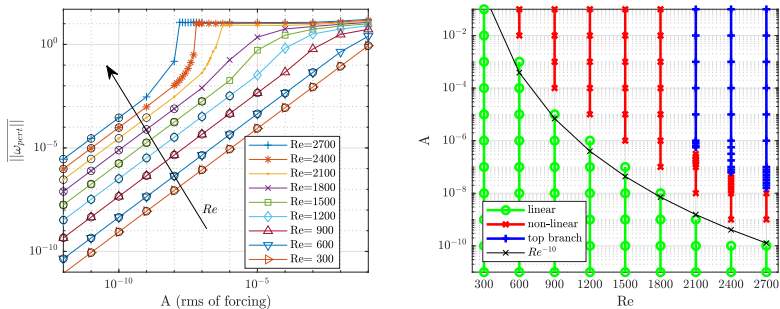
Comparison of linear and nonlinear time integration for $Re = 600$, numerical resolution R1. Top: perturbation azimuthal velocity u_θ at location ($r=5, z=0.9$) from linear (left) and nonlinear time integration (right). Bottom: Corresponding spectrum of non-linear (solid lines) and linear (dashed lines) at $z = 0.9$ for various r .



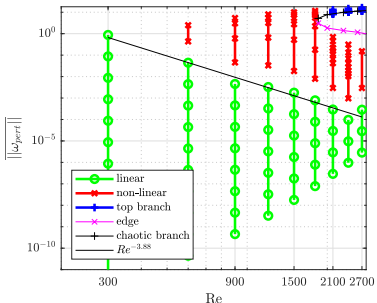
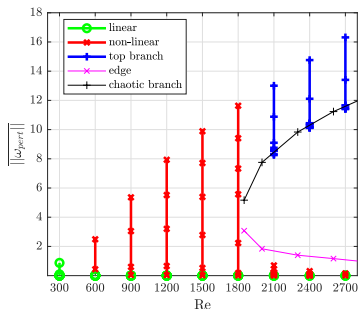
Comparison of linear and nonlinear time integration for $Re = 2100$, numerical resolution R1. Top: perturbation azimuthal velocity u_θ at location ($r=5, z=0.9$) from linear (left) and nonlinear time integration (right). Bottom: Corresponding spectrum of non-linear (solid lines) and linear (dashed lines) at $z = 0.9$ for various r .



Global observable $\|\omega_{pert}\|$ in nonlinear time integration at $Re = 2100$ for varying forcing amplitude A . The values of A are indicated both in the legend and in the plot for simplicity. Starting from $A = 10^{-7}$ nonlinear effects are observed. For $A \geq 10^{-6}$ the observable jumps to a different level corresponding to the presence of a non-trivial *top branch* solution.



Left: mean observable value $\|\omega_{pert}\|$ as a function of forcing amplitude A . The linear regime is indicated using open symbols whenever the slope of the line is at most 1% different from 1. For $Re \geq 2100$ the mean observable value level jumps to the top branch level for strong enough forcing amplitudes. Right: amplitudes corresponding to linear and nonlinear regime indicated respectively with green and red symbols. The top branch is reached for $Re > 1800$ whenever $\|\omega_{pert}\| > 5$.



Left: mean observable value $\|\omega_{pert}\|$ as a function of Re . The data corresponding to the chaotic solutions from [?] are superimposed in respectively blue (top branch) and pink (for the edge branch). Same colour coding as in the previous figure. Right : same data plotted in logarithmic scales.

